

## EFFECT OF RAPID THERMAL ANNEALING ON Co/Si/W/Si MULTILAYERS

A. Anopchenko<sup>1</sup>, M. Jergel<sup>1</sup>, E. Majková<sup>1</sup>, Š. Luby<sup>1</sup>, R. Senderák<sup>1</sup>, V. Holý<sup>2</sup>

<sup>1</sup>*Institute of Physics, Slovak Academy of Sciences, Dúbravská cesta 9, 842 28 Bratislava, Slovakia*

<sup>2</sup>*Laboratory of Thin Films and Nanostructures, Faculty of Science, Masaryk University, Kotlářská 2, 611 37 Brno, Czech Republic*

### 1. Introduction

Multilayer structures composed of a heavy refractory metal and a light spacer element are advantageously used in X-ray and ultraviolet optics. A crucial problem to be solved is a degradation of these structures under adverse ambient conditions like thermal loading in intense plasma source diagnostics or in synchrotron storage ring beamlines. The degradation takes place through interdiffusion and/or mixing at the interfaces the quality of which is decisive for obtaining high specular reflectivity.

In previous papers (e.g. [1]), we addressed the problem of thermal stability on W/Si multilayers. In this paper, we examine an alternative solution of increasing their thermal stability, namely an addition of Co layers. Considering the thermodynamic parameters of both Co- and W-silicides formation, we have assumed that the Si layers will react predominantly with Co when increasing temperature thus leaving the W/Si interfaces untouched.

### 2. Experimental

The samples were prepared by UHV electron beam deposition in UMS 500 Balzers apparatus onto oxidized Si(100) substrates. The sequence of the Si/Co/Si/W layers starting from the substrate was repeated 5 times. The first layer of Si was divided and the half of it was deposited onto the surface of the multilayer stack to avoid surface tarnishing. Two multilayers with smaller (MLS1) and larger (MLS2) nominal layer thicknesses (for the real ones see Table 1), as controlled by a quartz monitor, were prepared. In MLS1, the Co, W, and Si layers were found amorphous by X-ray diffraction (XRD) while in MLS2, the Co layers exhibited a poorly developed hcp phase.

The rapid thermal annealing (RTA) of the samples was performed in a halogen lamp vacuum furnace at the vacuum of  $10^{-3}$  Pa at a temperature of 500 °C for 30 s.

The interfaces were studied by X-ray reflectometry and diffuse scattering measurements at grazing incidence on a STOE high-resolution diffractometer.  $\text{CuK}\alpha_1$  radiation was provided by a double-crystal GaAs monochromator working at the 400 reflection in parallel non-dispersive arrangement with both crystals cut under  $3^\circ$  with respect to the diffracting (100) plane. In this way, a compromise between sufficient spectral resolution and intensity was achieved. A NaI(Tl) scintillation counter was used.

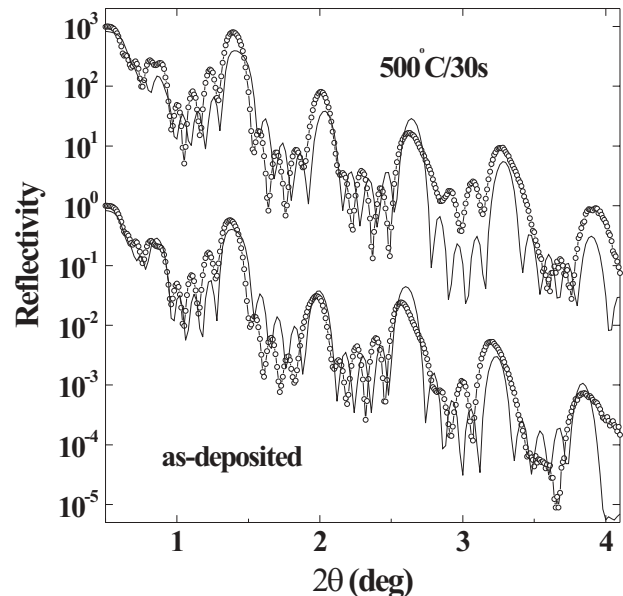


Fig. 1. Specular reflectivity of MLS1 before and after the RTA (circles) and its simulation (line) based on the Fresnel relations.  $2\theta$  is twice of the diffraction angle, i.e. the angle between the primary and secondary beams.

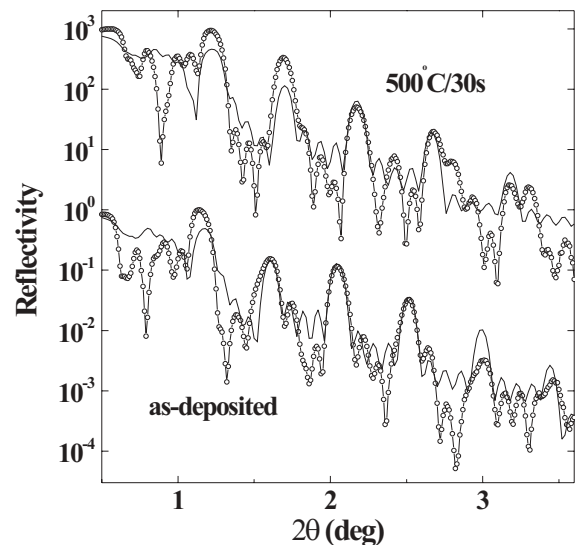


Fig. 2. Specular reflectivity of MLS2 before and after the RTA (circles) and its simulation (line) based on the Fresnel relations.

### 3. Results and their evaluation

The measured and simulated reflectivity curves of MLS1 and MLS2 before and after RTA are shown in Fig. 1 and Fig. 2. The Bragg maxima coming from the multilayer periodicity and Kiessig fringes in between due to the multilayer thickness are clearly observable. The simulation were based on the Fresnel relations [2] with the interface



roughness incorporated at each interface by Debye-Waller-like attenuation factor  $\exp(-q_{j-1}q_j \sigma_j^2)$ ,  $q_{j-1}$  and  $q_j$  being the scattering vectors above and below the  $j$ th interface, respectively, and  $\sigma_j$  being the root-mean-square (rms) roughness of this interface. The specular part of the diffuse scattering was neglected in these simulations.

As the scattering vector is perpendicular to the interfaces during a reflectivity measurement, the lateral interface characteristics (along the interfaces) cannot be extracted from the specular reflectivity. Therefore, the non-specular scans at grazing incidence with a non-zero lateral component of the scattering vector are unavoidable to characterize the interfaces completely. We traced the distribution of the scattered intensity throughout the reciprocal space by sample (detector) scans with the detector (sample) fixed at different Bragg maxima and in between.

The evaluation of the non-specular intensity due to the diffuse scattering on rough interfaces, was done within a semikinematical approach to the distorted-wave Born approximation (DWBA) [3]. Here, a semiinfinite substrate is taken as the ground state and the whole multilayer including roughness is taken as the disturbance. Such an approach accelerates calculations considerably and is fully justified in the absence of secondary scattering effects. To express the disturbance potential, both lateral and vertical correlations of the interface profiles have to be described. The lateral correlation was described by the self-correlation function

$$C_j(x) = \sigma_j^2 \exp\left(-\frac{x}{\xi_j}\right)^{2h_j} \quad (1)$$

where  $\xi_j$  is the lateral correlation length and  $h_j$  is a fractal parameter. For the description of vertical interface correlation, the correlation function

$$C_j^k(x) = \sqrt{C_j(x)C_k(x)} L(|z_j - z_k|) \quad (2)$$

was used with

$$L(q_x, z_j - z_k) = \exp\left(-\frac{q_x^2 |z_j - z_k|}{\alpha}\right) \quad (3)$$

or

$$L(z_j - z_k) = \exp\left(-\frac{|z_j - z_k|}{L_{vert}}\right) \quad (4)$$

i.e. dependent on (Eq. 3) and independent of (Eq. 4) the interface roughness frequency  $q_x$  which causes the lateral wave vector transfer  $q_x$  at the scattering process. Let us denote the frequency-dependent and frequency-independent models of the vertical interface correlation A and B, respectively. While model A directly follows from the microscopic thin film growth model proposed by Kardar, Parisi, and Zhang (KPZ model) [4], model B is rather phenomenological. The parameter  $\alpha$  in model A controls the degree of the correlation ( $\alpha \rightarrow \infty \Rightarrow$  total correlation,  $\alpha = 0 \Rightarrow$  no correlation) while  $L_{vert}$  in model B is directly vertical correlation length.

The simulations of the sample scans of MLS1 taken at the 1<sup>st</sup> Bragg order for both models of the vertical interface correlation are compared in Fig.3. Generally, the simulations with model A were slightly better but the difference was not very large. In Fig. 4 and Fig. 5, a comparison of the as-deposited and thermally treated sample MLS1 is shown for the sample and detector scans, respectively, taken at the 2<sup>nd</sup> Bragg order. A broad background due to the constructive interference of the diffusely scattered X-rays on conformal (vertically correlated) interfaces is seen in the sample scans and corresponds to additional non-specular maxima visible in the detector scans (resonant diffuse scattering [5]). Such a direct evidence of, at least partial, vertical interface correlation is observable also on as-deposited and thermally treated MLS2 (Fig.6 and Fig.7).

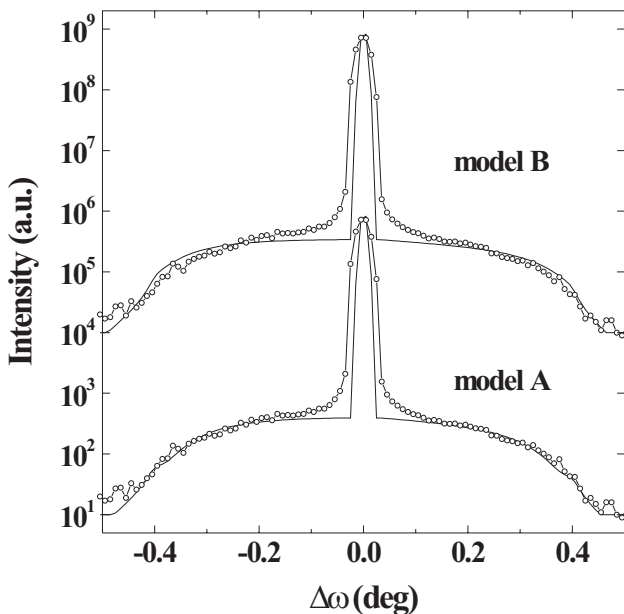


**Fig. 3.** Comparison of the simulation results for models A and B for the sample scan taken at the 1<sup>st</sup> Bragg order for the as-deposited MLS1.  $\Delta\omega$  means an offset from the specular position.

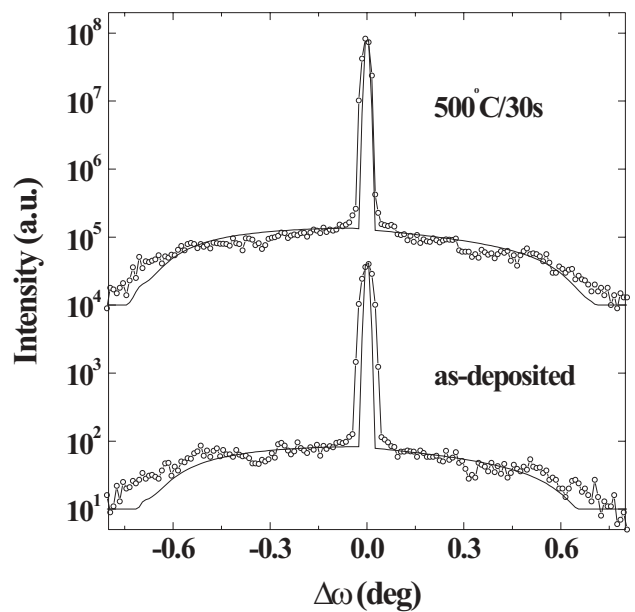


**Fig. 4.** Sample scan around the 2<sup>nd</sup> Bragg order for MLS1 before and after the RTA (circles) and its simulation (line) using model A.

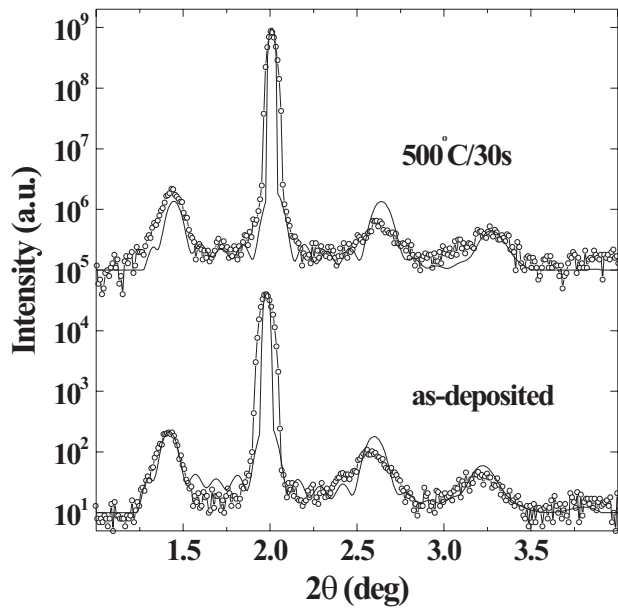


Fig. 5. Detector scan around the 2<sup>nd</sup> Bragg order for MLS1 before and after the RTA (circ.) and its simulation (line) using model A.

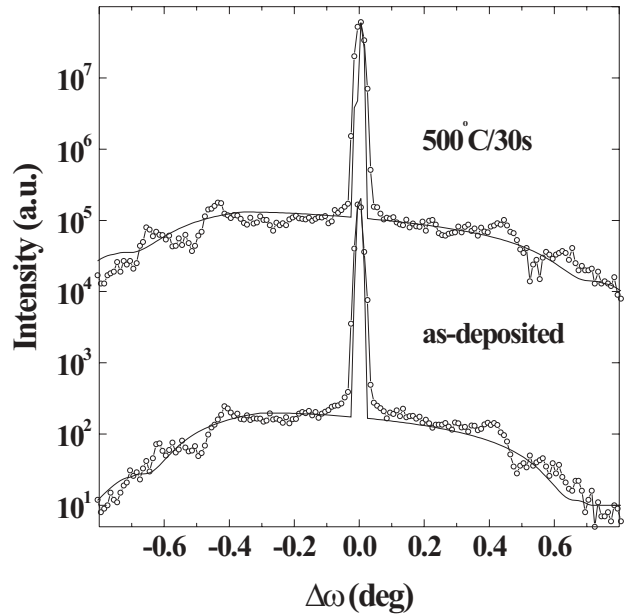


Fig. 6. Sample scan around the 3<sup>rd</sup> Bragg order for MLS2 before and after the RTA (circ.) and its simulation (line) using model A.

#### 4. Discussion

The Si layer thickness required for the formation of final  $\text{CoSi}_2$  and  $\text{WSi}_2$  disilicide phases is 3.64 nm and 2.53 nm per 1 nm of metal, respectively. The final silicide thicknesses are 3.52 nm for  $\text{CoSi}_2$  and 2.58 nm for  $\text{WSi}_2$  [6]. With regard to Si requirements, the conditions for silicide formation after a complete annealing connected with a degradation of the multilayer structure are better fulfilled in MLS1. Our magnetization measurements published elsewhere [7] have shown that there is no magnetic phase in as-deposited MLS1 which points to a considerable interdiffusion and intermixing leading to a silicide formation already before the RTA. This is contrary to MLS2 where continuous ferromagnetic Co layers could clearly be detected. Therefore, it may be expected that the multilayer stack is more affected by the RTA in MLS2.

The simulation parameters are gathered in Table 1. It may be seen that while the Co and Si layer thicknesses are sensitive to the RTA performed, the W layer ones are rather untouched. This result is consistent with the formation of Co silicides at lower temperatures than W silicides. On the other hand, the absolute changes of the Co and Si layer thicknesses due to the RTA are different in MLS1 and MLS2. Namely the Si layer thicknesses decrease more while the Co layer ones increase less in MLS2 which results into much larger reduction of the multilayer period in MLS2. This reduction in both samples may be ascribed to the annealing-out of the excess free volume inherent to amorphous structures.

The process induced by RTA may be viewed as the diffusion of primarily Si into the Co layers. Si is known as faster diffusion species in the Co/Si couple. Consequently,

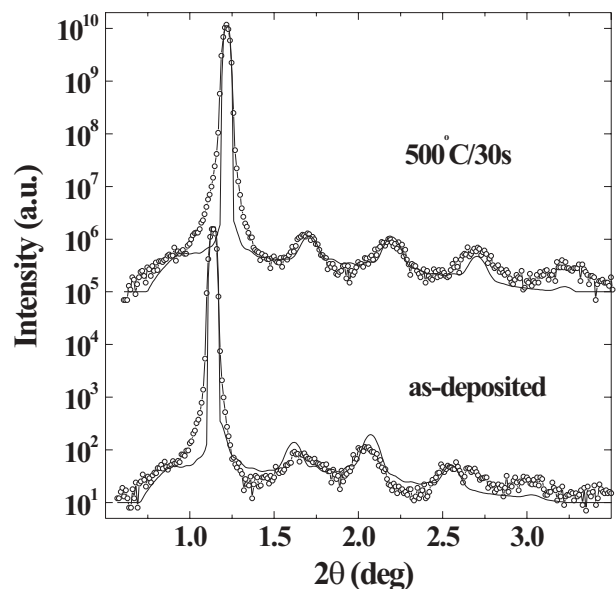


Fig. 7. Detector scan around the 1<sup>st</sup> Bragg order for MLS2 before and after the RTA (circ.) and its simulation (line) using model A.

**Table 1.** The simulation parameters obtained from the specular and non-specular scans.  $d_x$  and  $d$  denote the individual layer thicknesses and multilayer period, respectively. Other parameters are explained in the text.

Sample		$d_{\text{Si}}$ [nm]	$d_{\text{Co}}$ [nm]	$d_{\text{Si}}$ [nm]	$d_{\text{W}}$ [nm]	$d$ [nm]	$\sigma$ [nm]	$\xi$ [nm]	$\alpha$ [nm <sup>-1</sup> ] ( $L_{\text{vert}}$ [nm])
MLS 1	as-dep.	5.1	2.1	5.1	1.6	13.9	0.65	20	0.02(50)
	anneal.	4.5	3.1	4.5	1.6	13.7	0.60	20	0.02(50)
MLS 2	as-dep.	5.4	3.8	6.9	2.0	18.1	0.70	100	0.035(90)
	anneal.	4.7	4.2	6.1	2.0	17.0	0.80	60	0.035(90)



the interfaces shift backward into the Si layers and the Co layers get more and more “polluted” by Si so that they may be described as  $\text{Co}+\text{Co}_x\text{Si}_y$ . Namely,  $\text{Co}_2\text{Si}$  traces were observed for both RTA treated samples by XRD. This conclusion is supported by the fact that lower decrements of the refractive index than for pure Co had to be used when simulating the results from the RTA treated samples. A similar interface shift within a well preserved multilayer stack was evidenced in W/Si multilayers [8]. It follows from our results that such an interface shift in MLS1 does not change either the lateral or vertical correlations of the interface profiles while in MLS2, where much larger reduction of the multilayer period is observed, the interface shift occurs at larger distances and reduces the lateral correlation length by  $\approx 50\%$ . As the vertical correlation length is not changed due to the RTA both in MLS1 and MLS2, the same type of shift may be supposed for all Co-on-Si and Si-on-Co interfaces. This process is accompanied by the annealing-out of the excess free volume and, in the case of MLS2, by an increase of the rms interface roughness. In MLS1, this roughness even slightly decreases on the RTA which was observed also on some other metallic multilayers in the first stages of a thermal treatment. Both lateral and vertical correlation lengths are smaller in MLS1 than in MLS2 where the individual layers are thicker. The fractal parameter  $h$  is equal to unity for all samples, i.e. no fractal behaviour of the interfaces was observed.

Comparing Eq.(3) and Eq.(4),  $L_{\text{vert}}=\alpha/q_x^2$  may be defined for model A, i.e. the vertical correlation length is dependent here on the frequency of the interface roughness  $q_x$ . In Table 2, vertical correlation lengths are calculated from this formula for the lateral wave vector transfer at the extremities of the sample scans around successive Bragg maxima. It is seen that higher frequency components of the interface roughness are much less vertically replicated which is due to the fact that lateral adatom mobility during the growth breaks predominantly the vertical correlation of all roughness components shorter than the lateral diffusion length. Model B may be successful in such cases where the vertical correlation length is larger than the sample thickness in the measured range of the roughness frequencies (i.e. lateral wave vector transfer). From Table 2 it follows that it is the case for the sample scan around the 1<sup>st</sup> Bragg maximum for MLS1 and around the 1<sup>st</sup> and 2<sup>nd</sup> Bragg maxima for MLS2. The simulations around higher order Bragg maxima using model B were quite satisfactory, too, as the most intense part of the scan close to the specular maxi-

**Table 2.** Vertical correlation lengths from model A for the interface roughness frequencies corresponding to the extremities of the sample scans around successive Bragg orders.

MLS1	$10^3 q_x$ [nm <sup>-1</sup> ]	8.764 (1 <sup>st</sup> )	19.943 (2 <sup>nd</sup> )	35.590 (3 <sup>rd</sup> )	56.830 (4 <sup>th</sup> )
	$L_{\text{vert}}$ [nm]	260	50	16	6.2
MLS2	$10^3 q_x$ [nm <sup>-1</sup> ]	5.664 (1 <sup>st</sup> )	12.699 (2 <sup>nd</sup> )	21.770 (3 <sup>rd</sup> )	33.825 (4 <sup>th</sup> )
	$L_{\text{vert}}$ [nm]	1090	217	73.8	30.5

um is decisive for a good fit. However, if the measurements are not taken in a broad interval of the lateral wave vector transfer, model B may be quite satisfactory but does not describe the reality in the whole frequency range. This is especially true for the detector scans where the spanned interval of the roughness frequencies is smaller than in the case of the sample scans.

## 5. Conclusions

We have studied thermal stability of Co/Si/W/Si multilayers exposed to the RTA by the hard X-ray reflectivity and diffuse scattering measurements at grazing incidence. Fresnel computational code and semikinematical modification of the DWBA were used to simulate the experimental curves. A thermally induced shift of the Co//Si interfaces connected with intermixing was observed, the W/Si interfaces being rather untouched. MLS1 with thinner layers exhibits intermixing already in the as-deposited state and thus is more thermally stable comparing to MLS2. Here, the main effects of the RTA performed are an increase of the interface roughness by 0.1 nm and reduction of the multilayer period by 1.1 nm, the vertical correlation of the interface profiles being reduced by  $\approx 50\%$ . This correlation reflects the growth dynamics of the multilayer during the deposition. The KPZ growth model with frequency dependent vertical replication of the interface profiles describes well the non-specular scans. A higher degree of the vertical interface correlation in thicker MLS2 has some implications for imaging applications of Co/Si/W/Si multilayer mirrors where it is an unwished phenomenon. Further studies on Co/Si/W/Si multilayers RTA treated up to the collapse of the multilayer stack are in progress.

## Acknowledgement

*This work was partly supported by the Slovak Grant Agency (VEGA), project No. 5083/98.*

## References

1. M. Jergel, V. Holý, E. Majková, Š. Luby & R. Senderák, *J. Appl. Cryst.*, **30** (1997) 642-646.
2. J.H. Underwood & T.W. Barbee, *AIP Conf. Proc.*, **75** (1981) 170-178.
3. M. Jergel, V. Holý, E. Majková, Š. Luby, R. Senderák, H.J. Stock, D. Menke, U. Kleineberg & U. Heinzmann, *Physica B*, **253** (1998) 28-39.
4. M. Kardar, G. Parisi & Y.C. Zhang, *Phys. Rev. Lett.*, **56** (1986) 869-873.
5. V. Holý & T. Baumbach, *Phys. Rev.*, **B 49** (1994) 10668-10676.
6. S. P. Murarka: *Silicides for VLSI applications*, New York 1983. Academic Press.
7. E. Majková, B. George, Ch. Bellouard, Š. Luby, M. Jergel, R. Senderák & J. Babinský, *J. Magn. & Magn. Mat.*, **165** (1996) 415-416.
8. M. Jergel, Z. Bochniček, E. Majková, R. Senderák & Š. Luby, *Appl. Phys. Lett.*, **69** (1996) 919-921.

